Journal of Power Sources 266 (2014) 433–439

Contents lists available at ScienceDirect

Journal of Power Sources

journal homepage: www.elsevier.com/locate/jpowsour

Ultrathin ZnO coating for improved electrochemical performance of $LiNi_{0.5}Co_{0.2}Mn_{0.3}O_2$ cathode material

Ji-Zhou Kong [a, b, c, d, *], Chong Ren [a], Guo-An Tai [a], Xiang Zhang [a], Ai-Dong Li [d], Di Wu [d], Hui Li [d], Fei Zhou [a, b, c, *]

[a] State Key Laboratory of Mechanics and Control of Mechanical Structures, Nanjing University of Aeronautics and Astronautics, No. 29 Yudao Street, Nanjing 210016, PR China
[b] College of Mechanical and Electrical Engineering, Nanjing University of Aeronautics and Astronautics, Nanjing 210016, PR China
[c] Jiangsu Precision and Micro-Manufacturing Technology Laboratory, Nanjing 210016, PR China
[d] National Laboratory of Solid State Microstructures, Materials Science and Engineering Department, Nanjing University, Nanjing 210093, PR China

HIGHLIGHTS

- Ultrathin coating is deposited via ALD with high conformality and atomic scale thickness control.
- Ultrathin amphoteric oxide ZnO coating layer is amorphous.
- NCM-523 coated with 8 ZnO layers exhibits the significantly improved electrochemical performance.
- Ultrathin coating layer can protected the active material from the dissolution and HF attack.

GRAPHICAL ABSTRACT

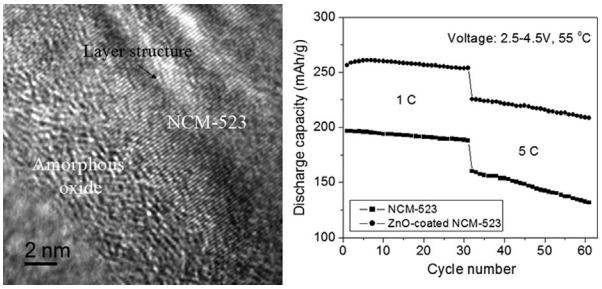

ARTICLE INFO

Article history:
Received 27 January 2014
Received in revised form
24 April 2014
Accepted 12 May 2014
Available online 20 May 2014

Keywords:
Lithium-ion battery
Cathode material
Ultrathin coating
Amorphous oxide
Electrochemical property

ABSTRACT

To enhance the electrochemical performance of $LiNi_{0.5}Co_{0.2}Mn_{0.3}O_2$ cathode, especially at elevated temperature, atomic layer deposition (ALD) technology has facilely used to deposit an ultrathin amorphous ZnO coating onto $LiNi_{0.5}Co_{0.2}Mn_{0.3}O_2$ with precise thickness-control at atomic scale. The coated cathode material with 8 ALD cycles exhibits the significantly improved discharge capacity and cycleability, as compared with those of the bare one. Such enhanced electrochemical performance of the coated sample is ascribed to its high-quality ultrathin amorphous ALD oxide coating, which can protect the active material from HF attack, reduce the dissolution of metal ions in the electrode and favor the lithium diffusion of the oxide proved by the electrochemical impedance spectroscopy (EIS) tests. The simple ALD process provides a potential new approach for the battery industry to fabricate novel electrodes with high performances even cycled at high rate at elevated temperature.

1. Introduction

Recently, layer-structured ternary material $LiNi_xCo_yMn_{(1-x-y)}O_2$ ($0 < x, y < 1$) with α-$NaFeO_2$ structure has been one of the most promising alternative cathode materials to replace $LiCoO_2$ in the next generation of the rechargeable lithium-ion battery (LIB) [1–4]. $LiNi_{0.5}Co_{0.2}Mn_{0.3}O_2$ is a representative kind of the nickel-rich ternary materials [5–7] with a high initial discharge capacity

* Corresponding authors. State Key Laboratory of Mechanics and Control of Mechanical Structures, Nanjing University of Aeronautics and Astronautics, No. 29 Yudao Street, Nanjing 210016, PR China. Tel./fax: +86 (0)25 84893083.
E-mail addresses: kongjzh@nuaa.edu.cn, kongjzh@163.com (J.-Z. Kong), fzhou@nuaa.edu.cn (F. Zhou).

http://dx.doi.org/10.1016/j.jpowsour.2014.05.027
0378-7753/

approximately 200 mAh g^{-1}. While the interfacial stability between the electrode and electrolyte must be improved in order to achieve the long-term stability and meet the safety requirements [8]. Recently, surface coatings of the electrodes with the metal oxides [9,10], phosphates [11], fluorides [7], etc. deposited via the conventional wet-chemical methods such as sol–gel techniques have been explored to improve the performance of LIB for vehicular applications. However, sol–gel methods require large quantities of solvents as well as multiple complex steps [12]. Meanwhile, the resulted coating layers lack the conformality, uniformity, and completeness [13]. Fortunately, the scalable ALD technique can precisely control the conformal coatings with Å-level thickness [14,15]. Therefore, the ultrathin ALD film doesn't disrupt the original electrical pathways constructed between the components in the electrode, reduce the overall capacity [13]. And it also allows for a high rate of Li-ion diffusion [16].

In this study, we deposit ultrathin and highly conformal ZnO coatings onto $LiNi_{0.5}Mn_{0.3}Co_{0.2}O_2$ powders by using ALD technique with precise thickness about 8 layers. The electrochemical performances of bare and ZnO-coated samples have been measured, and the influence of ZnO coating layer on the rate capability and cycleability of cathode is also explored.

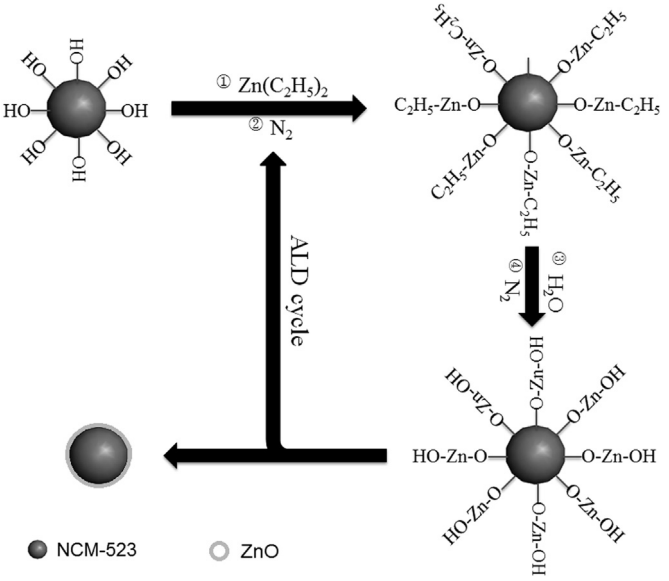

Fig. 1. Schematic illustration for ALD-ZnO growth on the surface of NCM-523 powder.

2. Experimental

Spherical precursor $Ni_{0.5}Co_{0.2}Mn_{0.3}(OH)_2$ was prepared by co-precipitation method using sodium hydroxide and ammonia as precipitator and complexing agent, respectively [7]. The precursor was mixed thoroughly with excess Li_2CO_3 in molar ratio of 1:1.06. The mixture was first heated at 500 °C for 4 h, and then calcined at 850 °C for 12 h in air to obtain the spherical $LiNi_{0.5}Co_{0.2}Mn_{0.3}O_2$ powders, marked as NCM-523.

Depositions of ZnO coatings on the particles were carried out in an atomic layer deposition system (Picosun SUNALE™ R-150B) using diethyl zinc $Zn(C_2H_5)_2$ and ultrapure grade H_2O as precursors with exposure time of 0.5 s, waiting time and purge time of 4 s, respectively. Vapors of two precursors were alternately carried by N_2 gas in a reaction chamber at 100 °C. Eight ZnO layers were coated on the cathode particles with via the corresponding ALD growth cycles.

The crystallographic structure of the prepared sample was examined by a powder XRD (Bruker D8 Advance) employing Cu Kα radiation. The morphology and microstructure of the samples were examined by TEM (Tecnai G^2 F20 S-Twin, FEI). Chemical composition of the coating was analyzed by XPS (Thermo ESCALAB 250) with Al Kα radiation, and all the spectra were calibrated by assigning the C 1s peak at 284.8 eV. The electrochemical experiments were carried out using 2025-type coin cells, with lithium foil as the anode electrode separated by the porous polypropylene film (Celgard 2700). The cathode electrode was composed of 80 wt% active material, 10 wt% carbon black, and 10 wt% PVDF binder. The electrolyte was a 1 mol L^{-1} $LiPF_6$ dissolved in ethylene carbonate, and dimethyl carbonate (EC:DEC = 1:1, *w*/*w*). The charge–discharge tests were galvanostatically performed at various C-rates (1C = 200 mA g^{-1}) in the potential range between 2.5 and 4.5 V. The electrochemical impedance spectroscopy (EIS) tests were carried out by an electrochemical workstation (CHI 660D), where an AC voltage of 5 mV amplitude was applied over the frequency range of 10 mHz–100 kHz at the charge state of 4.3 V. Before the EIS measurement, a 1 h hold was employed to ensure the constant voltage.

3. Results and discussion

The exceptional advantage is that ALD allows for the direct deposition on either individual electrode material particles or as-formed composite electrodes [12]. So ultrathin ZnO layer can be directly deposited onto the surface of cathode particles via ALD approach. As shown in Fig. 1, the schematic diagram is given to illustrate how the ALD ZnO coating is performed on powder. The sequential and self-limiting surface reactions of ALD lead to ZnO film growing monolayer by monolayer [14,17].

XRD patterns of the bare NCM-523 powders and NCM-523 particles coated with 8 ALD-ZnO layers are shown in Fig. 2. As expected in Fig. 2, all the diffraction peaks could be indexed in a hexagonal α-$NaFeO_2$ structure with a space group of R-3m, and no extra diffraction peaks about the related secondary phases or impurities exist. The splits of the (006)/(102) and (108)/(110) peak pairs for all samples indicate the formation of layered structure [5,7]. However, the ZnO phase is not detected, which could be ascribed to its amorphous state [17]. And the amorphous ZnO coating deposited by ALD causes minimal influence to the material structure. As is known, the integrated intensity ratio of $I_{(003)}/I_{(104)}$ is

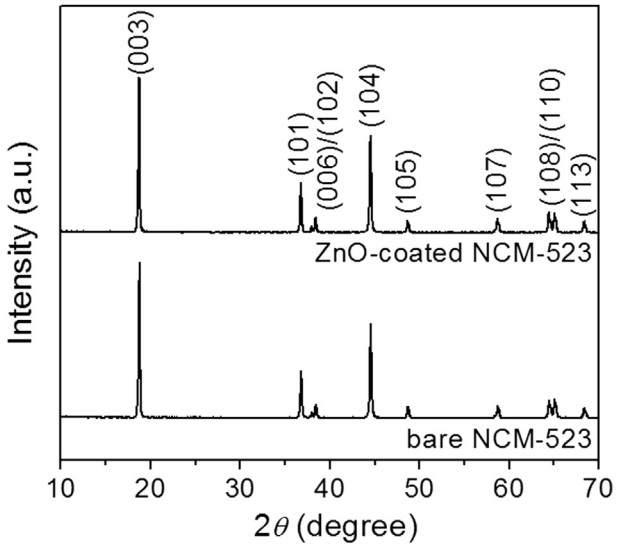

Fig. 2. XRD patterns of (a) bare NCM-523 powders and (b) NCM-523 particles with ALD-ZnO coating layer.

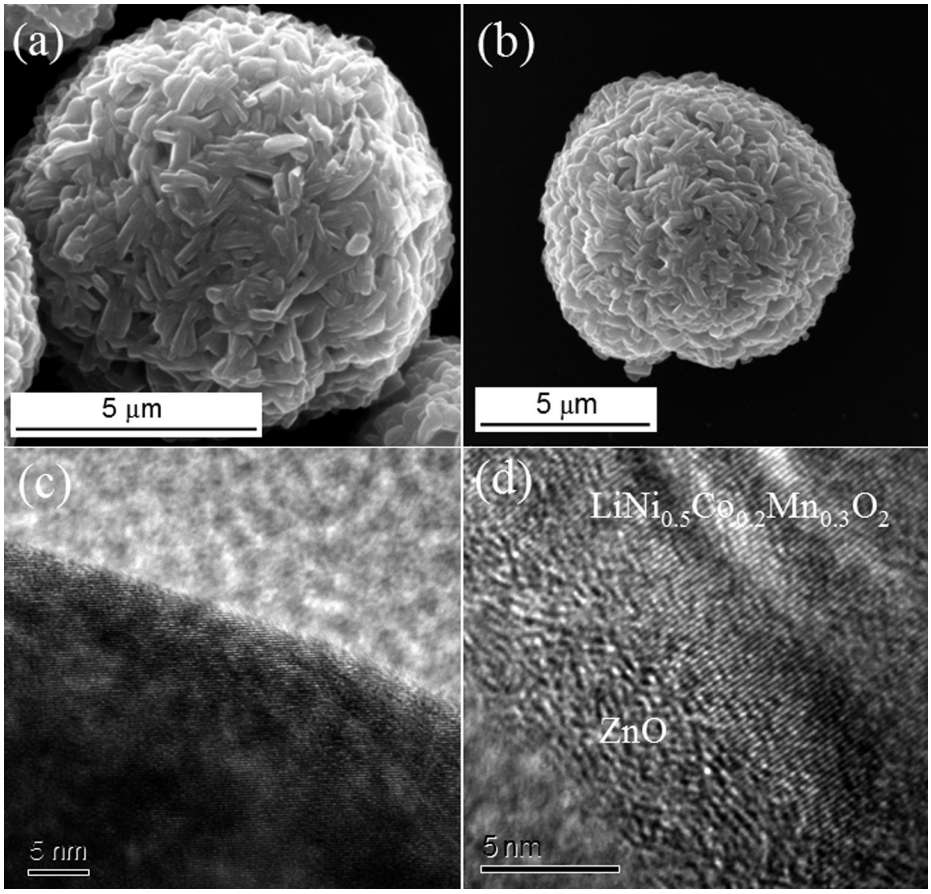

Fig. 3. (a) SEM and (b) TEM images of the bare NCM-523 particle, (c) SEM and (d) TEM images of the coated NCM-523 sample with 25 ZnO layers.

a sensitive parameter to determine the degree of cation mixing in the lattice. The values of $I_{(003)}/I_{(104)}$ are 1.63 and 1.59 for the bare and coated samples, respectively. Both ratios are larger than 1.2, which indicates a well-ordered α-$NaFeO_2$ structure with limited cation mixing.

Fig. 3 shows the morphology and composition of NCM-523 particles before and after the ALD-ZnO coatings. Fig. 3(a) shows the SEM image of the bare $LiNi_{0.5}Co_{0.2}Mn_{0.3}O_2$. It can be seen that the secondary particles show uniform spherical morphology with the average particle size of 8.5 μm, and each of the spherical secondary particles is made up of numerous primary grains. Fig. 3(b) and (c) show the high-resolution TEM (HRTEM) images of NCM-523 particles before and after ALD coating, respectively. The lattice fringe in the surface region for bare NCM-523 (Fig. 3(b)) is the well-ordered layered structure, which is identical to those in the centre region for the coated sample (Fig. 3(c)). In a typically wet-chemical procedure, e.g. sol–gel method, nonuniform agglomeration exists and the thick porous coating species is observed [15]. Compared with the HRTEM image of the bare NCM-523 (Fig. 3(b)), the 25 ALD-ZnO layers coated sample (Fig. 3(c)) exhibits the conformal ultra-thin coating layer with ~43.4 Å thickness which is clearly amorphous, quite different from the lattice fringes in the crystal region. Generally, the amorphous phase would favor the lithium diffusion due to its flexible structures [18]. The typical growth rate is calculated to be about 1.74 Å per cycle for ZnO, which is quite according with the results reported by Y. Wang et al. [17,19].

In order to confirm the ZnO coating layer deposited on NCM-523, XPS spectra were used to examine the surface of bare and ALD-ZnO coated NCM-523 cathodes. As shown in Fig. 4, the binding energies of Zn $2p_{3/2}$ of 1021.5 eV and $2p_{1/2}$ of 1044.3 eV are observed, which is assigned as the contribution the Zn–O chemical bond of ZnO. It demonstrates that the thin layer of ZnO exists on the surface of the NCM-523 particle. However, the Zn element is not detected on the bare cathode.

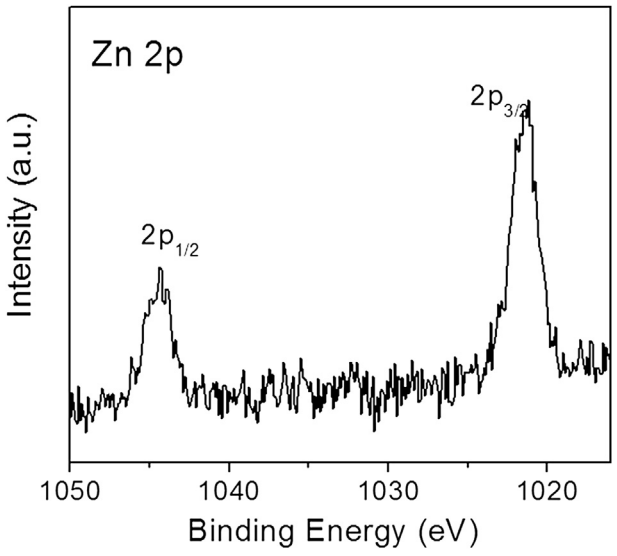

Fig. 4. XPS spectrum of Zn 2p of NCM-523 particle coated with 8 ZnO layers.

Fig. 5 shows the initial charge–discharge profiles of the pristine and ZnO-coated NCM-523 electrodes at 20 mA g^{-1} (C/10) between 2.5 and 4.5 V. All of the curves display a typical electrochemical behavior without an apparent voltage plateau. The first charge/discharge capacity, irreversible capacity and initial Coulombic efficiency for the pristine and ALD-modified samples are given in Table 1. The initial charge and discharge capacities are 245.1, 201.2 mAh g^{-1} and 267.3, 238.1 mAh g^{-1} for the bare and ZnO-coated NCM-523, respectively. The initial discharge capacity and initial Coulombic efficiency of the oxide is enhanced after coating with ALD-ZnO layer as compared with those of the bare sample.

Rate capability of the bare and ZnO-coated NCM-523 samples tested at 25 °C is shown in Fig. 6. The cells were charged/discharged at 0.1C–5C for every five cycles, then charged/discharged at 0.1C. As can be clearly seen from Fig. 6, the ZnO-coated electrode exhibits a superior rate capability than the bare one. For example, the ALD-ZnO coated NCM-523 discharged an acceptable capacity of 198.5 mAh g^{-1} at 1C and 148.2 mAh g^{-1} at 5C, retaining 83.5% and 62.4% of the original 237.6 mAh g^{-1} at 0.1C. While the pristine sample delivered only 163.3 mAh g^{-1} at 1C and 113.1 mAh g^{-1} at 5C. Above results reveal that the rate capability of $LiNi_{0.5}Co_{0.2}Mn_{0.3}O_2$ could be enhanced by ZnO ultra-thin coating, which maybe ascribes to the decrease of polarization [20].

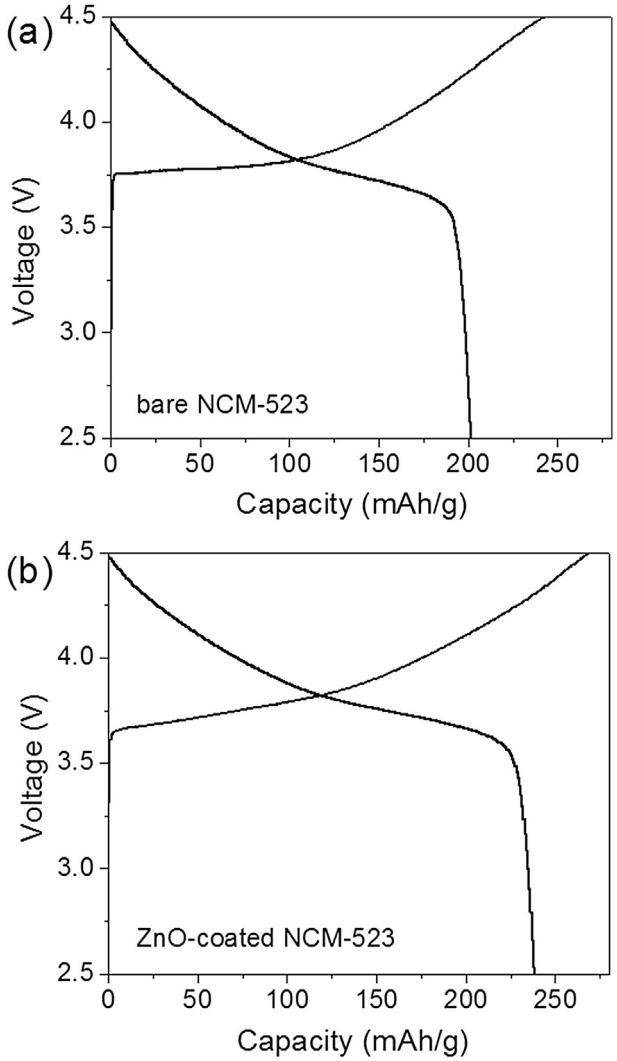

Fig. 5. Initial charge–discharge curves of the bare and ZnO-coated NCM-523 electrodes at 25 °C.

Table 1
Electrochemical data of the layered $LiNi_{0.5}Co_{0.2}Mn_{0.3}O_2$ before and after ALD-ZnO coating modifications.

Samples	Initial charge capacity (mAh g^{-1})	Initial discharge capacity (mAh g^{-1})	Irreversible capacity (mAh g^{-1})	Initial Coulombic efficiency (%)
Bare	245.1	201.2	43.9	82.1
ZnO-coated	267.3	238.1	29.1	89.1

The influence of ALD-ZnO coating on the cycling performance of NCM-523 was also investigated. Fig. 7 exhibits the discharge capacities versus cycle numbers for the Li/pristine and ultrathin ZnO-coated NCM-523 cells. At low current density (0.2C), both samples show good cycleability about 100% after 20 cycles. However, at high C-rate, the capacity retention of ZnO-coated sample is 91.5% after 60 cycles at 2C. While the pristine electrode shows a gradual decrease in discharge capacity, leading to the capacity retention of only 87.4% during the same cycling period. As is known, when the active material is charged to high voltage, the side reactions between the electrode and electrolyte result in forming some solid electrochemical inert layer, which hinders the diffusion of Li^+ and electron [21,22]. The conformal, self-limiting nature of ALD is attempted to coat the cathode material, such as $LiCoO_2$ [13], and $LiNi_{1/3}Mn_{1/3}Co_{1/3}O_2$ [23]. Amphoteric oxide ZnO deposited via ALD can effectively alleviate the dissolution of transition metal ions (especially the manganese ions) into the electrolyte by scavenging the harmful HF species through the formation of Zn–O–F and/or Zn–F layers [16,23] and retard the electrolyte decomposition by isolating the cathode particles from the electrolyte [24] which could explain in part the good capacity retention for ZnO-coated NCM-523 sample. At the same time, during the charge–discharge process, ultrathin ZnO coating layer does not block lithium ion diffusion into the cathode particles, and the crystal structural stability could be improved by surface coating when the cells tested at high voltage [18].

The cycling performances of the bare and ZnO-coated electrode were also investigated over 2.5–4.5 V at elevated temperature 55 °C. As shown in Fig. 8, the uncoated electrode suffers from fast capacity fading, especially at high C-rate, due to the side reactions between the electrode and electrolyte and the dissolution of transition metal ions caused by the attack from the acidic HF in electrolyte and electrolyte decomposition driven by high oxidation

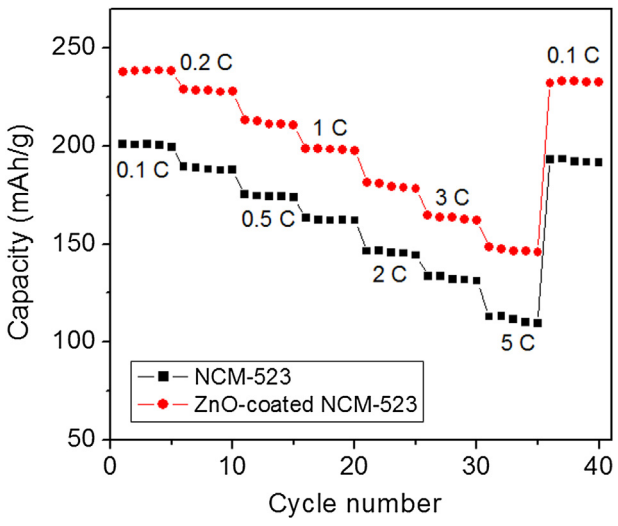

Fig. 6. Rate capability of the bare and ZnO-coated NCM-523 electrodes at 25 °C.

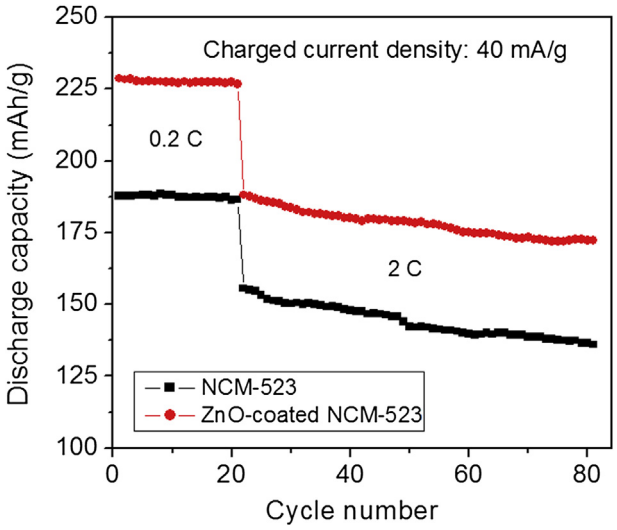

Fig. 7. Cycle performance of the bare and ZnO-coated NCM-523 electrodes at room temperature 25 °C.

activity during the high-potential charge/discharge [13]. ALD-ZnO coated NCM-523 has a high discharge capacity of 256.7 mAh g^{-1} at 1C, over 30% higher than that of the bare sample. And it also delivers an improved capacity retention about 92.5% of the initial discharge capacity 225.5 mAh g^{-1} at 5C, while the bare one retains only 82.2% at the same condition. As a result, the ultrathin ZnO coating layer could distinctly improve the cycling performance of the cathode materials at elevated temperature.

In order to further evaluate the effect of ZnO ALD coating on NCM523 particles, the EIS measurements were carried out in this work. Before the AC impedance measurements, the cells were equalized for 10 h after cycling at 300 K. Fig. 9 (a) and (b) show the Nyquist plots of the bare and ALD-ZnO coated NCM-523 samples at the charge state of 4.3 V in the 20th, 50th and 100th cycle (100 mA g^{-1}). The corresponding equivalent circuit in Fig. 9(c) is used to give a quantitative result to further understand the effect of the modification layer. The shapes of all the Nyquist plots are similar. A small interrupt in the high frequency corresponds to the solution resistance R_s. There were two semicircles in the EIS for the

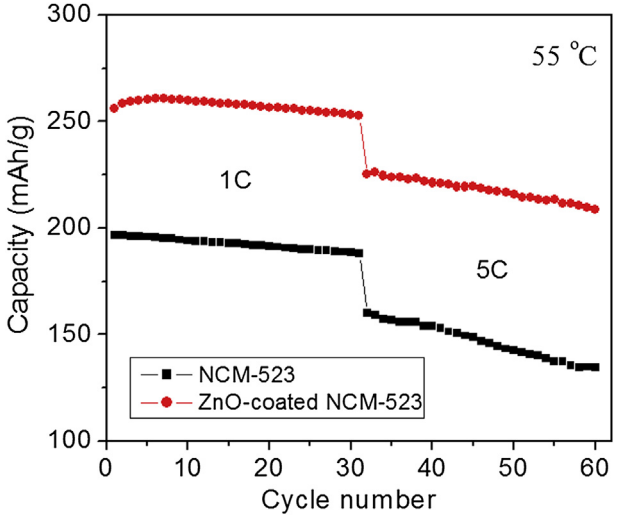

Fig. 8. Cycle performance of the bare and ZnO-coated NCM-523 electrodes at 55 °C.

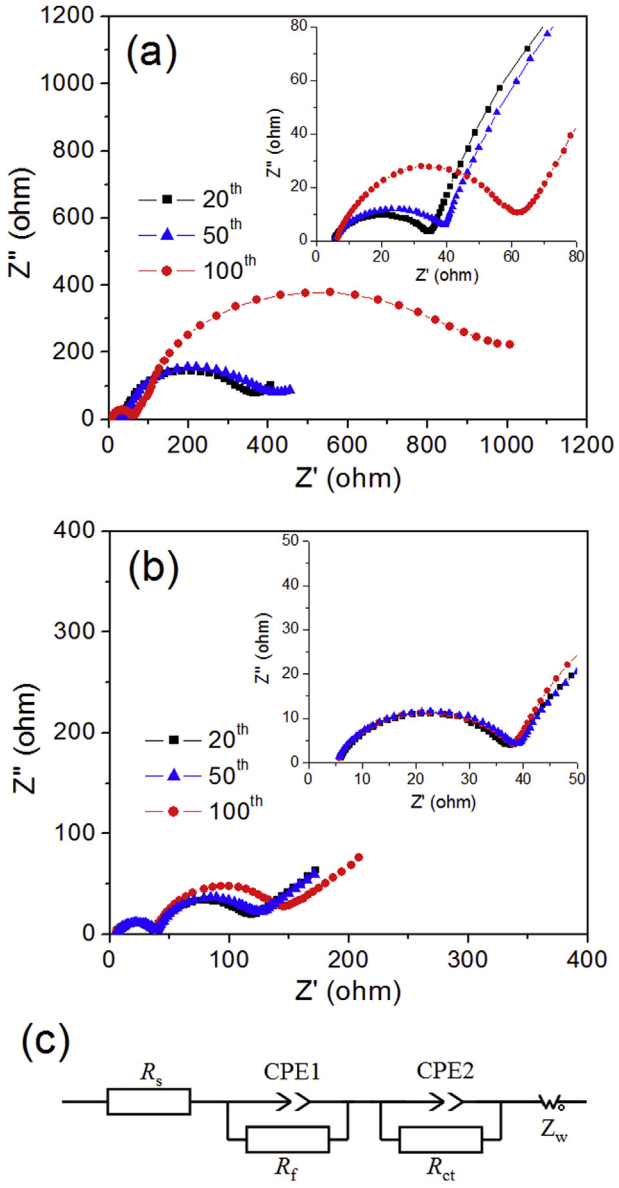

Fig. 9. Nyquist plots of (a) bare NCM-523 and (b) ZnO-coated NCM-523 electrodes at a charge state of 4.2 V for the 25th, and 50th cycle, (c) equivalent circuit performed to fit the Nyquist plots in (a) and (b).

electrodes. One in the high-to-medium frequency region is assigned to the impedance (R_f) of Li^+ diffusion in the surface layer (including the SEI film and the surface-modified layer). And the other in the low frequency region is attributed to the charge transfer resistance (R_{ct}) at the interface between the electrode and electrolyte. The quasi-straight line in the low frequency corresponds to Warburg impedance Z_w which refers to the impedance of Li^+ diffusion in bulk material [25,26].

For all samples, as listed in Table 2, the R_s values slightly changed during the cycling process. The R_s and R_f values of the bare NCM523 at the 20th cycle are 32.8 Ω and 90.4 Ω, respectively. After 100 cycles, it could be seen that the R_f and R_{ct} values increased during cycling for the bare one, particularly R_{ct}, which was dramatically added up to about 3 times of the value at the 20th cycle, so that the Warburg region becomes indistinguishable. For the coated sample, it shows that the coated sample delivers a similar R_s and a slightly smaller R_f with comparison to the bare one, which confirmed a

Table 2
The impedance parameters of equipment circuits.

Samples	Bare NCM-523			ZnO-coated NCM-523		
	R_s	R_f	R_{ct}	R_s	R_f	R_{ct}
20th	4.8	29.5	284.1	5.4	32.2	67.5
50th	5.9	55.3	332.6	4.9	34.4	70.4
100th	5.9	79.3	864.3	5.2	32.8	90.4

stable surface film after ALD-ZnO coating. In addition, the R_{ct} value remains stable as a function of cycle number when compared with the bare sample. After 50 cycles, it is only about 70.4 Ω, much smaller than that for the bare one. The steady value R_{ct} of ALD-ZnO sample can be explained as follows [25,26]: On one hand, the ALD-ZnO coating can stabilize the surface structure of NCM-523, and restrain the dissolution of the metal ions. On the other hand, better SEI film forms due to the ultrathin amorphous coating layer which would favor the lithium diffusion [18]. The EIS results prove the effect of ALD-ZnO coated layered NCM-523 again, and support the enhanced rate capability and cycling stability seen in Figs. 6 and 7.

Since the linear part in the low frequency of EIS is directly related to Li^+ diffusion in bulk electrode [25], we can calculate the diffusion coefficient of Li^+ to clarify the modification effect of ALD-ZnO coating using the following equation [27,28].

$$D_{Li^+} = R^2T^2 \Big/ 2A^2n^4F^4C^2\sigma^2 \quad (1)$$

Here R is the gas constant, T is the absolute temperature, A is the interface between the electrolyte and the active material, which is calculated on the basis of the BET area (0.763 $m^2\ g^{-1}$ for bare NCM-523), n is the number of electrons involved in reaction, F is the Faraday constant, C is the concentration of lithium ion and σ is the Warburg factor which is relative to the real resistance Z_{re}.

In the linear part of EIS, Z_{re} is the function of frequency (ω), and fit the following equation [21,29].

$$Z_{re} = R_s + R_{ct} + \sigma\omega^{-1/2} \quad (2)$$

In Eq. (2), K is a constant. From the plot of Z_{re} as a function of $\omega^{-1/2}$ shown in Fig. 10, the good linear relationships are obtained and the values of σ are calculated. Thus, according to Eq. (1), the diffusion coefficients of Li^+ is 4.56 × 10^{-9} $cm^2\ s^{-1}$ for the bare material with change after 20 cycles, which is close to the result reported by Wang et al. [30]. The corresponding D_{Li+} of ALD-ZnO coated sample is valued to 2.67 × 10^{-8} $cm^2\ s^{-1}$. The increase of Li^+ diffusion coefficient can be ascribed to the modification of the ultrathin amorphous ZnO coating layer.

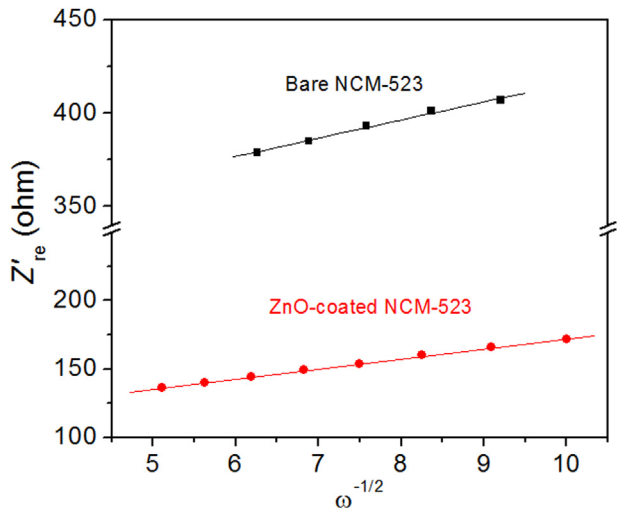

Fig. 10. Relationships between Z_{img} and $\omega^{-1/2}$ for the bare NCM-523 and ZnO-coated NCM-523 electrodes.

4. Conclusions and outlook

ALD technology has facilely used to deposit the ultrathin amorphous ZnO coating layer onto bare NCM-523 to enhance the electrochemical performance of electrode. The coated cathode material with 8 ALD layers exhibits the significantly improved discharge capacity and cycleability, especially at the elevated temperature, when compared with the bare one. Such enhanced electrochemical performance of the coated sample is ascribed to the high-quality ultrathin amphoteric oxide ZnO coating layer, which is high conformality and homogeneity. And it could prevent the active material from the metallic dissolution and HF attack, and improve the structural stability at high voltage. In addition, the ultrathin coating layer does not block lithium ion diffusion into the cathode particles during the charge–discharge process. The simple ALD process provides a potential new approach for the battery industry to fabricate the novel electrodes with high performances even cycled at high rate at elevated temperature.

Acknowledgment

This work is financially supported by "Jiangsu Province National Natural Science Fund Project", No. BK20130800; "the Fundamental Research Funds for the Central Universities", No. NS2014054; "the Opening Funding of National Laboratory of Solid State Microstructure", No. M25018; "Priority Academic Program Development of Jiangsu Higher Education Institutions (PAPD)", "the special fund of the scientific and technological achievements transformation project in Jiangsu province", No. BA2013142 and the Talent Program of Nanjing University of Aeronautics and Astronautics (NUAA) (2012). We would like to acknowledge them for the financial support.

References

[1] T. Ohzuku, Y. Makimura, Chem. Lett. 7 (2001) 642–643.
[2] S. Venkatraman, J. Choi, A. Manthiram, Electrochem. Commun. 6 (2004) 832–837.
[3] H.B. Ren, X. Li, Z.H. Peng, Electrochim. Acta 56 (2011) 7088–7091.
[4] Y.K. Sun, B.R. Lee, H.J. Noh, H.M. Wu, S.T. Myung, K. Amine, J. Mater. Chem. 21 (2011) 10108–10112.
[5] J.Z. Kong, H.F. Zhai, C. Ren, G.A. Tai, X.Y. Yang, F. Zhou, H. Li, J.X. Li, Z. Tang, J. Solid State Electrochem. 18 (2014) 181–188.
[6] D.C. Li, Y. Sasaki, M. Kageyama, K. Kobayakawa, Y. Sato, J. Power Sources 148 (2005) 85–89.
[7] K. Yang, L.Z. Fan, J. Guo, X.H. Qu, Electrochim. Acta 63 (2012) 363–368.
[8] Y.S. Jung, P. Lu, A.S. Cavanagh, C.M. Ban, G.H. Kim, S.H. Lee, S.M. George, S.J. Harris, A.C. Dillon, Adv. Energy Mater. 3 (2013) 213–219.
[9] Y.Y. Huang, J.T. Chen, F.Q. Cheng, W. Wan, W. Liu, H.H. Zhou, X.X. Zhang, J. Power Sources 195 (2010) 8267–8274.
[10] W. Liu, M. Wang, X.L. Gao, W.D. Zhang, J.T. Chen, H.H. Zhou, X.X. Zhang, J. Alloy. Compd. 543 (2012) 181–188.
[11] S.B. Kim, K.J. Lee, W.J. Choi, W.S. Kim, I.C. Jang, H.H. Lim, Y.S. Lee, J. Solid State Electrochem. 14 (2010) 919–922.
[12] Y.S. Jung, A.S. Cavanagh, L.A. Riley, S.H. Kang, A.C. Dillon, M.D. Groner, S.M. George, S.H. Lee, Adv. Mater. 22 (2010) 2172–2176.
[13] I.D. Scott, Y.S. Jung, A.S. Cavanagh, Y.F. Yan, A.C. Dillon, S.M. George, S.H. Lee, Nano Lett. 11 (2011) 414–418.
[14] S.M. George, Chem. Rev. 110 (2010) 111–131.
[15] J.Q. Zhao, G.Y. Qu, J.C. Flake, Y. Wang, Chem. Commun. 48 (2012) 8108–8110.
[16] M. Bettge, Y. Li, B. Sankaran, N.D. Rago, T. Spila, R.T. Haasch, I. Petrov, D.P. Abraham, J. Power Sources 233 (2013) 346–357.
[17] J.Q. Zhao, Y. Wang, J. Phys. Chem. C 116 (2012) 11867–11876.
[18] H.G. Song, J.Y. Kim, K.T. Kim, Y.J. Park, J. Power Sources 196 (2011) 6847–6855.
[19] J.Q. Zhao, Y. Wang, J. Solid State Electrochem. 17 (2013) 1049–1058.

[20] K. Yang, L.Z. Fan, J. Guo, X.H. Qu, Electrochem. Commun. 63 (2012) 363–368.
[21] J. Liu, Q.Y. Wang, B. Reeja-Jayan, A. Manthiram, Electrochem. Commun. 12 (2010) 750–753.
[22] S.J. Shi, Y.J. Mai, Y.Y. Tang, C.D. Gu, X.L. Wang, J.P. Tu, Electrochim. Acta 77 (2012) 39–46.
[23] L.A. Riley, S.V. Attac, A.S. Cavanagh, Y.F. Yan, S.M. George, P. Liu, A.C. Dillon, S.H. Lee, J. Power Sources 196 (2011) 3317–3324.
[24] M. Wohlfahrt-Mehrens, C. Vogler, J. Garche, J. Power Sources 127 (2004) 58–64.
[25] S.J. Shi, J.P. Tu, Y.Y. Tang, X.Y. Liu, Y.Q. Zhang, X.L. Wang, C.D. Gu, Electrochim. Acta 88 (2013) 671–679.
[26] S.J. Shi, J.P. Tu, Y.Y. Tang, Y.Q. Zhang, X.Y. Liu, X.L. Wang, C.D. Gu, J. Power Sources 225 (2013) 338–346.
[27] A.J. Bard, L.R. Faulkner, Electrochemical Methods, second ed., Wiley, 2001.
[28] Z. Li, F. Du, X.F. Bie, J. Phys. Chem. C 114 (2010) 22751–22757.
[29] J. Ni, H. Zhou, J. Chen, X. Zhang, Electrochim. Acta 53 (2008) 3075–3083.
[30] S.Y. Yang, X.Y. Wang, X.K. Yang, Y.S. Bai, Z.L. Liu, H.B. Shu, Q.L. Wei, Electrochim. Acta 66 (2012) 88–93.